

國立交通大學

奈米科技研究所

碩士論文

藉由不同粒徑奈米粒子證明免疫球蛋白辨識粒徑差



Accessing functional flexibility of immunoglobulin by  
nanoparticles- the size matters

研究生：陳昱勳 Yu-shiun Chen

學 號：9352512

指導教授：黃國華 博士 Dr.Guewha Steven Huang

中華民國九十五年六月

95

碩士論文

藉由不同徑米子  
奈米粒證明  
疫苗蛋白辨  
識粒差  
徑異性



交通大學

工學院  
奈米科技研究所

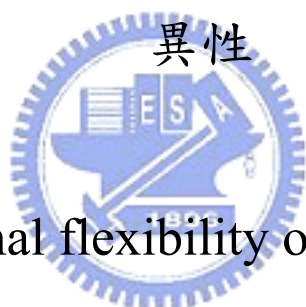
陳昱勳

國立交通大學

奈米科技研究所

碩士論文

藉由不同粒徑奈米粒子證明免疫球蛋白辨識粒徑差



Assessing functional flexibility of immunoglobulin by  
nanoparticles- the size matters

研究生：陳昱勳

Yu-shiun Chen

學號：9352512

指導教授：黃國華 博士

Dr. Guewha Steven Huang

中華民國九十五年六月

藉由不同粒徑奈米粒子證明免疫球蛋白辨識粒徑差異性

Accessing functional flexibility of immunoglobulin by nanoparticles- the size matters

研究生：陳昱勳

Student : Yu-shiun Chen

指導教授：黃國華博士

Advisor : Dr. Guewha Steven Huang

國立交通大學  
奈米科技研究所  
碩士論文



A Thesis  
Submitted to Institute of Nanotechnology  
College of Engineering  
National Chiao Tung University  
in partial Fulfillment of the Requirements  
for the Degree of  
Master  
in

Institute of Nanotechnology

June 2006

Hsinchu, Taiwan, Republic of China

中華民國九十五年六月

## 中文摘要

免疫球蛋白(IgG)具有彈性鉸鏈可以自由的旋轉與移動 Fab 片段和 Fc 片段。具備自由旋轉與移動的能力可以提供抗原抗體具備更佳的辨識能力。然而，用傳統的生物分子替代抗原，作為免疫球蛋白(IgG)辨識抗原決定部位的研究是有困難的，因為大多數的生物分子(例如:蛋白質)有結構的變化和序列辨識構造問題。因此我們提出一個假說應用不同粒徑大小的奈米金粒子(GNP)作為抗原抗體彈性辨識研究的引子，經由奈米金粒子(GNP)的使用可作為量測 Fab 片段與抗原結合彈性大小的一把尺。利用酵素連結免疫吸附分析進行實驗將抗 5 奈米金粒子(GNP)的抗血清和已結合 3.5 奈米、4.5 奈米、5 奈米、6 奈米、8 奈米、12 奈米、17 奈米金粒子(GNP)的表面進行分析。實驗結果發現 4.5 奈米與 5 奈米金粒子(GNP)與抗血清中蛋白有最大的結合，3.5 奈米與 6 奈米金粒子(GNP)與抗血清中蛋白有部分結合。然而，在 8 奈米或是更大粒徑的奈米金粒子(GNP)則無結合現象。雖然在免疫球蛋白(IgG)中的兩個 Fab 片段可以自由的旋轉與移動是已證實的結果，但經由我們的實驗結果發現免疫球蛋白(IgG)的鉸鏈當進行抗原辨識過程中彈性與自由度是受到限制的。

我們也同時證明奈米金粒子(GNP)與免疫球蛋白(IgG)複合體構造的關係。利用抗血清與 5 奈米奈米金粒子(GNP)和量子點(QD)共同沉澱，形成

IgG(QD-IgG)進而形成 GNP-IgG-QD 複合體經由低溫電子顯微鏡進行觀察。經由穿透式電子顯影鏡證實 GNP-IgG-QD 結合在一起形成三個一組。經由量測結果得知 GNP-IgG-QD 的夾角範圍由 35 度到 120 度，由上述結果應證了 Fab-Fc 具有彈性鉸鏈。總結上述實驗結果我們發現在 Fab 片段進行抗體抗原辨識過程是彈性是受到限制的，而 Fab-Fc 的彈性是比較大的。

關鍵字: 免疫球蛋白、奈米金粒子、穿透式電子顯影鏡



# Abstract

Immunoglobulin contains flexible hinges that allow free rotation and movement of Fab and Fc fragments. This free rotation and movement would provide broader search for the antibody-antigen recognition; however, the flexibility of immunoglobulin regarding the epitope binding is difficult to measure using traditional biomolecules as antigen. This is in parts due to the dynamic and sequence-specific structure of most biomolecules, i.e. protein. The hypothesis underlined the current study is to probe the flexibility of antigen-antibody recognition by applying a wide range of gold nanoparticles (GNPs). The collection of GNPs thus will serve as molecular ruler to measure the functional flexibility of Fab fragment upon searching for antigen. Enzyme-Linked Immunosorbent Assay (ELISA) was performed using anti-5 nm GNP antiserum to bind microwells coated with 3.5 nm, 4.5 nm, 5 nm, 6 nm, 8 nm, 12 nm, and 17 nm GNPs. Maximal binding was observed at 4.5 nm and 5 nm GNPs. Partial binding activity was observed for 3.5 nm and 6 nm GNP. Nevertheless, the antiserum does not bind to 8 nm or larger GNPs. Although free rotation and movement of the two Fab fragments are expected, our result indicated that the hinges allowed only a very limited freedom during the antigen recognition process.

We also examined structure of GNP-immunoglobulin complex. The antiserum was co-precipitated with 5 nm GNP and quantum dots-conjugated IgG (QD-IgG) to form a GNP-IgGs-QD complex and examined under cryo-electron microscopy. EM image confirmed the composition of GNP-immunoglobulins-

QD trio. The obtained angles of GNP-immunoglobulins-QD ranged from 35 to 120 degrees which indicated that the flexibility of Fab-Fc hinge was comparable to previous reports. In summary, during the antibody-antigen recognition the Fab arms showed only a very limited flexibility while Fab-Fc shows much bigger degrees of freedom.

Keywords: Immunoglobulin; Enzyme-Linked Immunosorbent Assay (ELISA); gold nanoparticles





Chinese Abstract	.....	i
Abstract	.....	iv
List of Figures	.....	vii
Chapter 1	Introduction .....	1
Chapter 2	Review .....	3
2 . 1	Gold nanoparticles.....	3
2 . 2	Water-based gold nanoparticle synthesis .....	7
2 . 2 . 1	Advantages.....	7
2 . 2 . 2	Disadvantages.....	8
2 . 3	Solution-based synthesis of gold nanoparticles.....	8
2 . 3 . 1	Advantages.....	9
2 . 4	Immunoglobulin G .....	11
2 . 5	Enzyme-linked immunosorbent assay.....	14
2 . 3 . 2	Disadvantages.....	15
Chapter 3	Materials and Methods.....	15
3 . 1	Preparation gold nanoparticles .....	15
3 . 2	Enzyme-Linked Immuno-Sorbent Assay (ELISA).....	16

3 . 3	Competition ELISA.....	17
3 . 4	Electron Microscopy.....	18
Chapter 4	Result and Discussion .....	19
4 . 1	Antiserum specific to 5 nm gold nanoparticle...	19
4 . 2	EM imaging of GNP immunoglobulin Quantum Dots conjugate.....	25



# List of Figures

<b>Fig. 2.1</b>	Absorption spectra of colloids obtained at various reaction temperatures .....	5
<b>Fig. 2.2</b>	SEM image of the gold nanoparticles synthesized by microwave heating .....	5
<b>Fig. 2.3</b>	Absorption spectra of colloids obtained at various citrate concentrations .....	6
<b>Fig. 2.4</b>	Five sols of colloidal gold prepared in water and in mixtures of butyl acetate and CS <sub>2</sub> .....	10
<b>Fig. 2.5</b>	Structure of an intact IgG1K for phenobarbital .....	12
<b>Fig. 3.1</b>	Enzyme-Linked Immuno-Sorbent Assay (ELISA) .....	17
<b>Fig. 4.1</b>	Survival number for mice immunized with gold nanoparticles .....	20
<b>Fig. 4.2</b>	LC <sub>50</sub> measured by MTT assay of NIH-3T3 cellculture .....	21
<b>Fig. 4.3</b>	Competition ELISA for the binding of anti-5 nm GNP antiserum and 5 GNP .....	23
<b>Fig. 4.4.1</b>	The control experiment exhibited pair-wise particles identified as QD-IgG which might co-precipitated mouse IgG .....	26
<b>Fig. 4.4.2</b>	Each trio was composed of 3 basic components: a grey protein mass of immunoglobulins, a 5 nm GNP and a 3 nm QD .....	26
<b>Fig. 4.4.3</b>	Higher magnification displayed a GNP-IgGs-QD .....	27

	conformation.....	
<b>Fig. 4.4.5</b>	To obtain the GNP-(IgGs)-QD angle a ball-and-stick model was proposed .....	28
<b>Fig. 4.5</b>	Schematic drawing for ball-and-stick model.....	31
<b>Fig. 4.6</b>	Stereo view of 3D plots for the measured angle and distances of GNP-IgGs-QD complexes .....	34
<b>Fig. 4.7</b>	Projection of apparent angle and distances of GNP-IgGs-QD complexes on the theoretical $\theta_0$ plane .....	35



# Chapter 1 Introduction

## Introduction

Immunoglobulin G (IgG) is a Y-shaped molecule composed of two types of fragments: Fab fragments form the two arms and Fc fragment forms the stalk of Y. Crystal structures of intact IgGs: human IgG1, murine IgG1, and murine IgG2a, have been solved by X-ray diffraction analysis [1]. Each Fab is connected to Fc by a flexible hinge of 12 to 19 amino acids. The hinge allows structural flexibility in the crystal: the Fab arm rotates as much as 158°; the Fab-Fc angle ranges from 66° to 123°; and the Fab-Fab angle ranges from 115° to 172° [2]. Electron microscopy observed up to 180° of rotation for Fab respect to Fc [3]. Three-dimensional structures of monoclonal IgG determined by cryo-electron tomography shows that there is large degree of freedom for both Fab-Fab hinge and Fab-Fc hinge in solution. This flexibility would allow the IgG molecules a broader range to search for antigens. Although the hinges potentially allow fragments to freely move and rotate, it is yet to be determined how does this flexibility contribute to the antigen recognition.

By convention proteins of different size can serve as ruler to measure the dynamics of Fab-Fab angle. This has been demonstrated by analyzing antibody binding to lysozyme, ovalbumin, and bovine serum albumin [4]. By measuring the molar ratio of antigen versus antibody, it was concluded that in solution Fab segments present sufficient flexibility that promotes simultaneously binding to two proteins each 5 to 9 nm of diameter. In particular, when the antibody is immobilized the flexibility is greatly restricted. However, the lack of structural characterization and the comparison of binding between different epitopes

weaken the exciting conclusion of this study.

Therefore, continuous measurement for the flexibility of immunoglobulin during antibody-antigen recognition is not easily achieved by conventional methodology. Applying biomolecule as antigen to probe the continuous space for immunoglobulin recognition encountered inevitable problem that the structure of biomolecule is sequence-specific. Designing a series of biomolecule which continuously change their sizes and at the same time conserve identical epitope is of practical difficulty. Nanoparticles, on the other hand, can be synthesized at desired diameter in the nanometer range. With uniform surface to serve as antigen, a spectrum of nanoparticles is potentially a powerful ruler to measure the flexibility of antibody-antigen recognition. The hypothesis underlying the current study is to probe the flexibility of antigen-antibody recognition by applying a broad range of gold nanoparticles (GNPs). The collection of GNPs thus will serve as molecular ruler to measure the functional flexibility of Fab fragment during the search for antigen.

In this study, we synthesized various sizes of gold nanoparticles, in which diameter ranged from 3.5 nm to 37 nm. We obtained antiserum specifically recognizing 5 nm gold nanoparticle. The variety of size would serve as a me

# Chapter 2 Review

## 2.1 Gold nanoparticles:

Metal nanoparticles have attracted much attention in the past few years due to their potential for use as device elements in nanoelectronic and optical application. Successful fabrication of useful devices depends on the ability to prepare ordered assemblies of nanoparticles in a rapid and inexpensive manner.

The synthesis of nanoparticles with desired size/shape has, therefore, enormous importance, especially in the emerging field of nanotechnology. However, it is a fact that the reproducible preparation of stable particles with controlled prechosen size is a very difficult task using the popular colloid-chemical approach. This, in fact, demands development of a new general method as well as improvement over the existing ones. Among the known colloidal nanoparticles systems, gold is one of the most widely studied ones. And a few systematic approaches already exist to obtain particles of prechosen size via its controlled formation [5]. For example, Frens (1973) proposed a method where reducing/stabilizing agent, citrate to gold ratio was varied. This results in particles with a broad size range (diameters between 10 and 150 nm). But for more than 30 nm diameter particles the monodispersity was observed to be poor. Leff et al. (1995) synthesized gold particles with diameters ranging from 1.5 to 20 nm by varying the Au(III) ion to stabilizer thiol molar ratio. This approach requires long time, 12 h or so to allow the reaction products to attain equilibrium. Another methodology, known since 1906, is 'seed'- or 'germ'-mediated growth which promises to obtain particles of desired size [6]. Here, appropriate amounts of precursor ions are reduced over the preformed 'seed' or 'germ', i.e.,

small particles by suitable reducing agents. The reducing agent used in the second stage of 'seed'-mediated growth is generally a weaker one, viz.,  $\text{H}_2\text{NOH}$ , ascorbate ion. They should reduce only the precursor ions which are adsorbed onto the 'seed' surface without creating any new nucleation center. The final size of the particles would depend on the size of the 'seed' and the amount of the precursor ions to be reduced on them (Schmid, 1992). Therefore, in principle, the smaller is the starting seed, the lower will be the desired size limit of the particles. It allows preparing particles over a broad size range. Smaller particles are generally produced by using stronger reducing agents, viz.,  $\text{NaBH}_4$ , phosphorus, tetrakis (hydroxymethyl) phosphonium chloride, etc., or radiolytic method. Furthermore, nature of the particle stabilizer, solvent, reaction condition, viz., pH, temperature, etc., plays crucial role in determining the final size of the particles. Recently, a radiolytic and a chemical size control with improved monodispersity via seed-mediated growth of colloidal gold nanoparticles were reported by Henglein and Meisel and Natan's group (Brown & Natan, 1998; Brown et al., 2000), respectively. They have followed iterative growth method, i.e., particles were grown in the immediately previous step were used as seeds in the next growth step. In the present study, we examine the applicability of a combination of photochemical approach with a non-iterative growth method to develop a simple and fast technique of size control. Here, particles of various size ranging from average diameter 5 to 20 nm could be obtained within few minutes by UV irradiation at room temperature ( $28^\circ\text{C}$ ) in presence of air. Furthermore, larger size particles (diameter 25–110 nm) were produced directly from the original seed particles by varying the ratio of original [seed] to  $[\text{Au(III)}]$  and using ascorbic acid as reductant. It should be noted that ascorbate ion is frequently used as reducing agent for reduction of  $\text{Au(III)}$  or  $\text{Ag(I)}$  ions. Goia



and Matijevic (Goia et al., 1999) recently used isoascorbic acid at various pH conditions to synthesize relatively large spherical gold particles (ranging in modal diameter from 80 nm to 5m) directly from Au(III) ions.

[ 6-15 ]

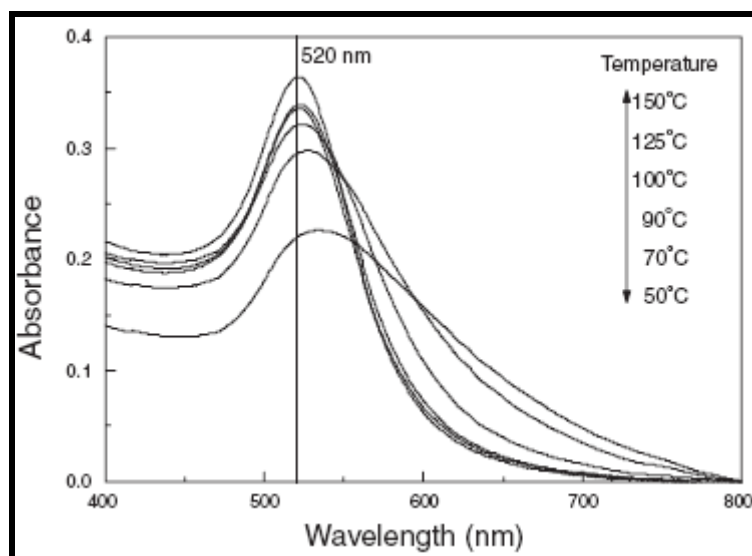


Fig. 2.1 Absorption spectra of colloids obtained at various reaction temperatures.

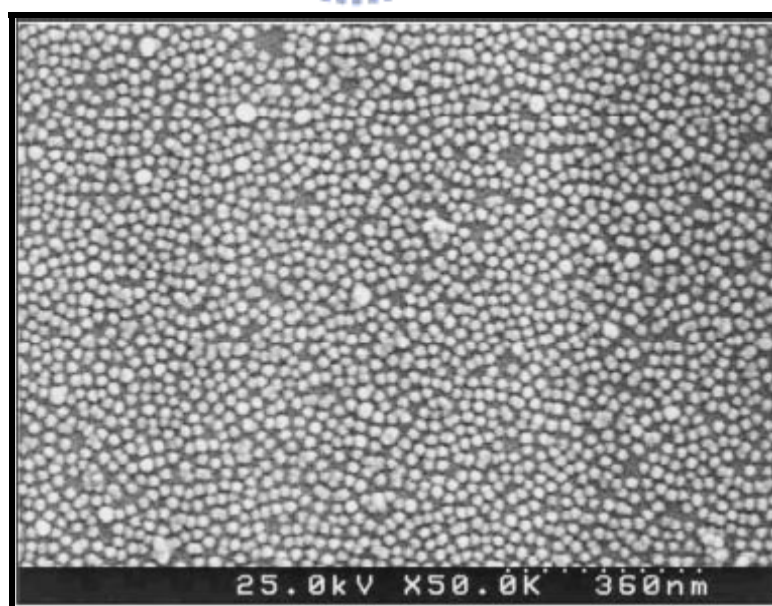
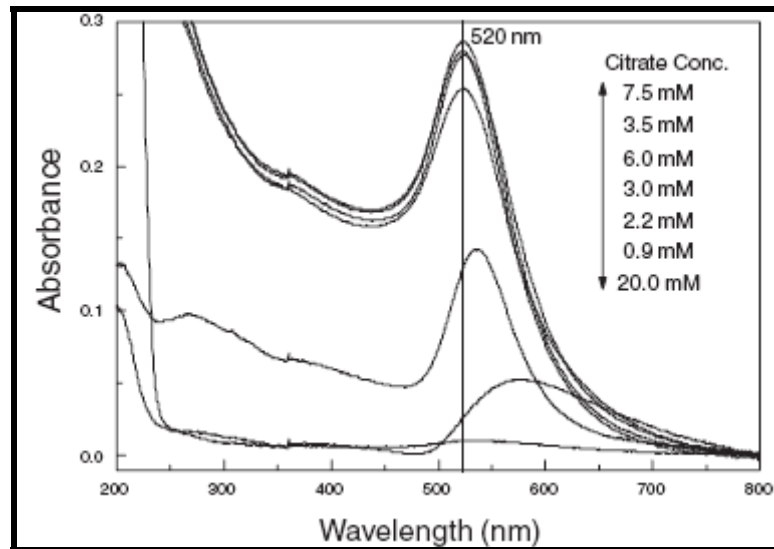


Fig. 2.2 SEM image of the gold nanoparticles synthesized by microwave heating. Gold nanoparticle preparation conditions: 10mL of aqueous solution containing

**3.5mM citrate and 1mM HAuCl<sub>4</sub>. Microwave irradiation operation conditions: 600W of applied energy, reaction temperature controlled at 125\_C with temperature increase speed at 80\_C/min and holding time for 15 min.**



**Fig. 2.3 Absorption spectra of colloids obtained at various citrate concentrations. The vertical arrow indicates the order intensity at 520nm with different citrate concentrations.**

## **2.2 Water-based gold nanoparticle synthesis**

### **2.2.1 Advantages:**

- Water is a good solvent for a number of metal ions as well as a variety of capping molecules. The synthesis involves preparation of an aqueous gold salt solution followed by reduction of the metal ions in a single step<sup>21</sup>. It is therefore considerably simpler than the multi-step Brust protocol.
- No additional stabilization against aggregation of the gold nanoparticles is required – surface bound ions (citrate ions, chloroaurate ions, etc.) stabilize the nanoparticles electrostatically in solution.
- Electrostatic layer-by-layer assembly involving, for example, oppositely charged polyelectrolytes/surfactants and nanoparticles may be readily accomplished on suitably functionalized surfaces.
- Nanoparticle shape control can be easily effected by using suitable micelles (arising due to spontaneous assembly of suitable surfactants in water) as templates.
- Perhaps the biggest advantage of a water-based synthesis procedure is that bioconjugation of the gold nanoparticles with DNA<sup>19</sup>, enzymes<sup>46</sup>, etc. may be easily accomplished. [ 15-21 ]

### **2.2.2 Disadvantages:**

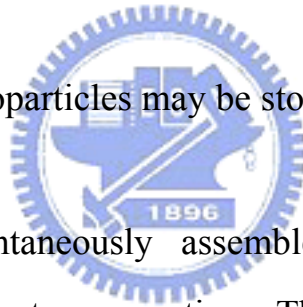
- Ionic interactions limit the concentration of gold nanoparticles in the aqueous phase to very dilute levels, a big drawback in biological labeling of the nanoparticles.
- Control over the particle size and monodispersity in a particular reduction protocol is not very good.

- The gold nanoparticles do not spontaneously assemble into a close-packed hexagonal arrangement on solvent evaporation.
- The gold nanoparticles are not easily separated from solution in the form of a powder that would be readily re-dispersible in water after storage.

## **2.3 Solution-based synthesis of gold nanoparticles**

### **2.3.1 Advantages:**

- High degree of control may be exercised over the gold nanoparticle size, monodispersity<sup>29</sup> and chemical nature of the nanoparticle surface (via capping with terminally functionalized thiols)
- High concentrations of the gold nanoparticles in solution may be easily prepared.
- Functionalized gold nanoparticles may be stored as a powder without sintering of the particles.
- The nanoparticles spontaneously assemble into closepacked, hexagonal monolayers upon solvent evaporation. The collective properties of the nanoparticle assembly may be controlled by varying the interparticle separation via capping with different chain length alkanethiols.



### **2.3.2 Disadvantages:**

- The procedure is a multi-step one involving independent phase transfer of the gold ions followed by their reduction and capping.
- While close-packed monolayers of the gold nanoparticles may be deposited by solvent evaporation, there is little control over the process of assembly. Furthermore, superlattices of the gold nanoparticles cannot be readily deposited, in contrast with the layer-by-layer assembly that is possible for electrostatically stabilized gold nanoparticles in water.

– Formation of bioconjugates with gold nanoparticles is not possible in an organic environment. It is clear that both methods for the synthesis of gold nanoparticles have characteristic advantages. Depending on the particular application of the nanoparticles, the ideal condition would be to somehow marry the two methods and thus maximize their advantages. This may be conveniently done by effecting a phase transfer of gold nanoparticles synthesized in one medium (water/organic solvent) to the second medium (organic solvent/water). In addition to maximizing the benefits accruing from a combination of the two syntheses methods, the ability to move nanoparticles across liquid interfaces into environments of specific physicochemical properties to probe, for example, variation in the optical properties of the nanoparticle solution<sup>49</sup> is an attractive feature of phase transfer protocols. In the remaining part of this article, I discuss some of the methods developed to carry out the phase transfer of gold nanoparticles in both directions.



**Figure 2.4 Five sols of colloidal gold prepared in water and in mixtures of butyl acetate and CS<sub>2</sub>.**



## **2 . 4 Immunoglobulin G**

Two intact IgG molecules with genetic hinge deletions have been analyzed by X-ray diffraction. Both of these myeloma proteins, Dob and Mcg, were conformationally constrained as a consequence of missing hinge polypeptides.

The structure of another, Kol, was a normal immunoglobulin with an intact hinge, but the Fc was crystallographically disordered and could not be visualized. In all cases the antibodies exhibited global 2-fold symmetry for the visible components.

Recently, the structure of an intact IgG2a was determined which had no overall symmetry (Harris et al., 1992, 1997). That anti-canine lymphoma Mab contained two independent, local dyads, one relating Fab constant domains and the second relating heavy chains in the Fc. The two dyads were obliquely oriented and non-intersecting.

The intact murine IgG1K (Mab 61.1.3), described here, is specific for the anti-epileptic drug phenobarbital. The crystals were monoclinic space group P21 with one entire molecule as the asymmetric unit. No crystallographic obligation existed for the Mab to possess exact global symmetry, suggesting that the IgG1 might exhibit a considerable degree of segmental flexibility, as The residue numbering convention for the entire paper is that of Kabat et al. (1991).

Atomic coordinates are deposited with the Brookhaven Protein Data Bank using this same numbering system. Abbreviations used: IgG, immunoglobulin G; Mab, monoclonal antibody; CDR, complementarity determining region; NCS, non-crystallographic symmetry. J. Mol. Biol. (1998) Academic Press Limited for the IgG2a. Based on fluorescent depolarization studies, IgG1 is known, however, to be the most rigid of the four mouse subclasses [ 20-28 ]



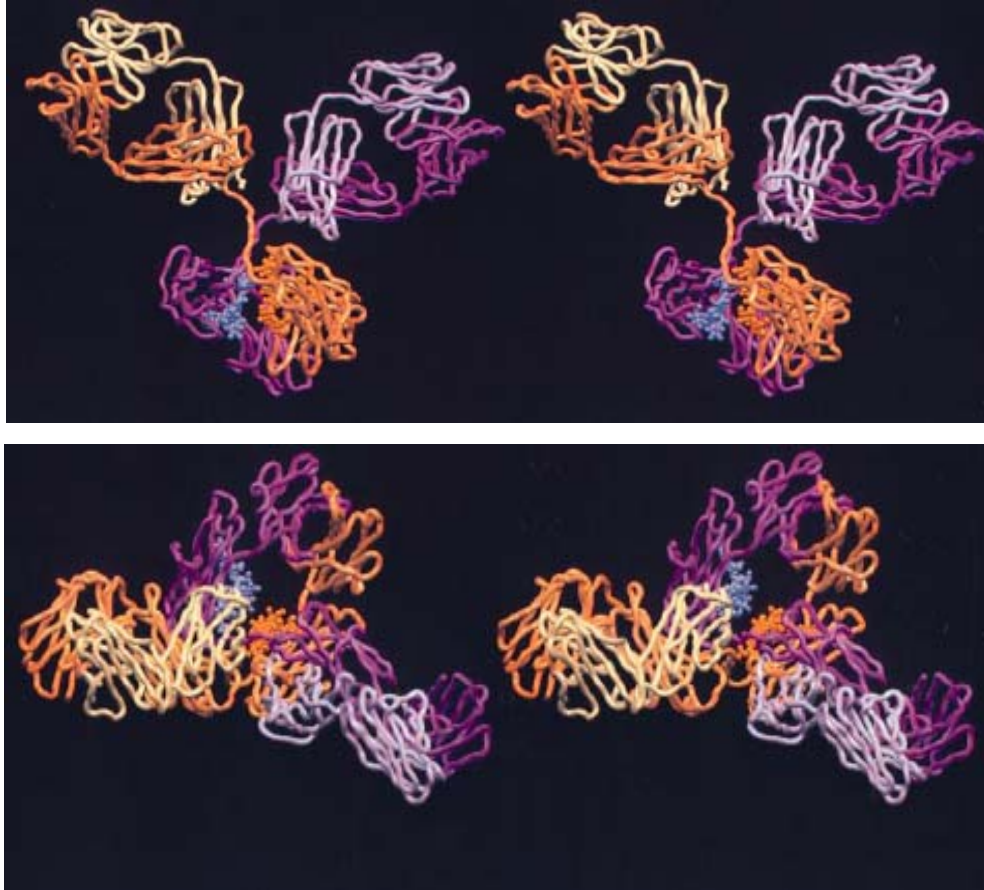


**Figure 2.5 Structure of an intact IgG1K for phenobarbital. Light chain1 is in pink, heavy chain1 in magenta, light chain2 in yellow, and heavy chain2 in orange. In (a) the IgG1 is viewed perpendicular to the approximate dyad axis relating Fab segments. The 2-fold rotation is near exact, but Fabs are translated by 9 Å with respect to one another along the rotation axis. In (b) the IgG1 is viewed perpendicular to the pseudo 2-fold axis relating heavy chains of the Fc segment. The angle between the Fab and Fc dyads is 107°, thus the long axis of the Fc is dislocated and roughly at a right angle to the plane of the Fabs. Hinge angle differences are evident here as well. The Fc segment of the IgG1 lies in the crystallographic xz plane, with its dyad approximately along the face diagonal.**





## **2.5 Enzyme-linked immunosorbent assay**

The enzyme-linked immunosorbent assay (ELISA) has been shown to be a highly sensitive technique capable of detecting antibodies to a wide variety of antigens (4-6, 8-10, 13, 18). This technique has the following advantages: the enzyme conjugates and the substrate reaction products are stable for long

periods of time, results can be read visually or on a spectrophotometer, and ELISA lacks the potential radiation hazards of radioimmunoassay. In this report an ELISA technique is used to measure relative amounts of isotypically specific antibodies against the lipopolysaccharide (LPS) extracted from a hybrid of *Shigella flexneri* and *Escherichia coli* (*Shigella* X16). The ELISA technique used in this study is a modification of our earlier procedure which did not directly relate the absorbance units from the substrate reaction to specific antibody against *Shigella* X16 LPS (X16 LPS) in gravimetric terms (13, 18). Data from the present study (i) establish sensitivity and specificity of the technique, (ii) assess parameters affecting the ELISA system, and (iii) compare this ELISA to passive hemagglutination and quantitative precipitation by using immunoglobulin G (IgG) fractions from rabbit antisera to X16 LPS. [ 29-34 ]

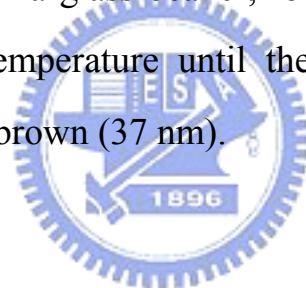


## Chapter 3 Materials and Methods

Materials.  $\text{HAuCl}_4$ , sodium citrate,  $\text{NaBH}_4$ ,  $\text{HCl}$ ,  $\text{HNO}_3$ ,  $\text{H}_2\text{SO}_4$ , and  $\text{H}_2\text{O}_2$  were purchased from Sigma-Aldrich and Fisher.  $\text{H}_2\text{O}$  was  $>18 \text{ M}\Omega$  from a Milli-Q water purification system. Quantum dots-conjugated anti-mouse IgG was purchased from Invitrogen (USA)

### **3.1 Preparation gold nanoparticles**

The seed colloids were prepared by adding 1 mL of 0.25mM HAuCl<sub>4</sub> to 90 mL of H<sub>2</sub>O and stirred for 1 min at 25 °C. Two milliliters of 38.8 mM sodium citrate was added to the solution and stirred for 1 min followed by addition of 0.6 mL freshly prepared 0.1 M NaBH<sub>4</sub> in 38.8 mM sodium citrate. Different diameters of gold nanoparticles ranging from 3.5 nm to 12 nm were generated by changing the volume of seed colloid added. The solution was stirred for an additional 5 to 10 min at 0 to 4 °C (Brown, Walter, Natan, 2000, Chem Mater, 12, 306-313). Fifty microliters of 0.1M ascorbic acid, 9mL growth solution (0.25mMHAuCl<sub>4</sub>, 0.08M cetyltrimethylamonium bromide), and 1.0mL Seed colloid (8.0±0.8nm in diameter) was combined in a glass beaker, followed by continuous stirring for 10 to 20 min at room temperature until the solution turned reddish brown (approximately 17 nm) or brown (37 nm).



### **3.2 Enzyme-Linked Immuno-Sorbent Assay (ELISA)**

Each microwell of the 96-well Corning plate was pre-treated with 100µL 2% Glutaraldehyde for 20 min at room temperature. One hundred and 50 microliters of 15 mM gold nanoparticles were added to the microwells and incubated for 2 hour at room temperature followed by Milli Q water wash for three times and then washed with 0.5% Triton X-100 in PBS for three-times. Blocking for non-specific binding was performed by adding 100uL of 3% BSA and incubated

for 60 min at room temperature followed by PBS wash for three times. Binding was performed by adding 100uL properly diluted antiserum into microwells and incubated for 1 hr at room temperature followed by thoroughly washes. HRP-conjugated anti-mouse IgG, ABTS, and H<sub>2</sub>O<sub>2</sub> was incorporated in sequence to the wells according to manufacture's protocol and the binding efficiency was monitored by absorbance at 405 nm.



### **3.3 Competition ELISA**

Competition ELISA was performed as described previously. In short, the competing reaction was performed in an ependorf tube by adding gradually concentrated competitor to the anti-5 nm gold nanoparticle anti serum in a total volume of 100  $\mu$ L, incubated 1 hr at room temperature, and used as antiserum following the previously described ELISA procedure.

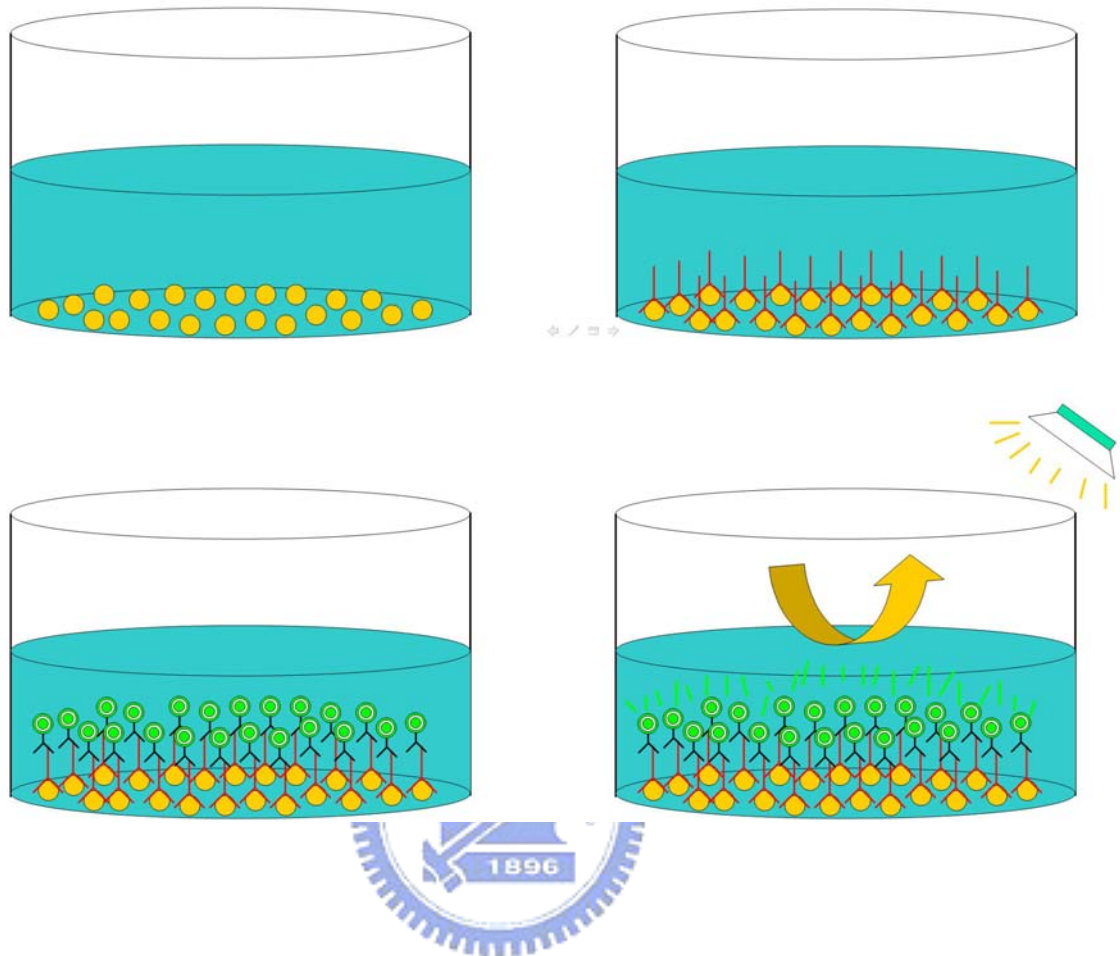


**Fig.3.1 Enzyme-Linked Immuno-Sorbent Assay (ELISA)**

### **3 . 4 Electron Microscopy**

The specimen was deposited onto copper wire and snap-frozen in the liquid nitrogen. After staining with iodine, the EM examination was performed using JEM-2010 Electron Microscope (JEOL Ltd., Japan) under the specified condition. The molecular model of immunoglobulin was constructed using the crystal structure of IgG2 retrieved from NCBI and with Rasmol graphing software (<http://www.umass.edu/microbio/rasmol/>) The molecular model of

immunoglobulin was constructed using the crystal structure of IgG2 retrieved from NCBI and with Rasmol graphing software.



## Chapter 4 Results and Discussion

### 4.1 Antiserum specific to 5 nm gold nanoparticle

We synthesized 5 nm, 8 nm, 12 nm, 17 nm, and 37 nm GNPs according to the published procedure [1]. The synthesis of GNP was monitored by UV absorbance and the size was examined by electron microscopy. To obtain antibodies specifically recognizing GNP BALB/C mice were immunized by weekly intra-peritoneal injection of adjuvant-emulsified 5 nm, 8 nm, 12 nm, 17 nm, and 37 nm GNPs. Mice injected with 8 nm, 12 nm, 17 nm, or 37 nm GNP died within 2 weeks, while mice injected with 5 nm GNP were feeble but

survived at the end of the fourth week (Figure 4.1). It is unexpected that GNPs of larger size were lethal but not 5nm GNP. To investigate the origin of toxicity GNPs were incorporated into the growth media of NIH 3T3 cell culture. Colorimetric methyl-thiazol-tetrazolium (MTT) assay was performed to measure  $LC_{50}$  for GNPs.  $LC_{50}$  ranged from 0.3 to 0.4 mM with 5 nm GNP presenting the most toxic effect to cultured cells (Figure 4.2). Thus the difference in animal survival rate might be unrelated to the cytotoxicity of GNPs.

We obtained antiserum from the 5 nm GNP-immunized mice. Enzyme-Linked Immunosorbent Assay (ELISA) was performed to measure the binding activity of anti-5 nm GNP antiserum against 3.5 nm, 4.5 nm, 5 nm, 6 nm, 8 nm, 12 nm, and 17 nm GNP-coated wells (Figure 2). Both control serum and antiserum withdrawn from 12 nm GNP-injected mice (harvested at the second week) showed no reactivity. The anti-5nm GNP antiserum showed significant binding activity to 3.5 nm, 4.5 nm, 5 nm, and 6 nm GNPs but none to GNPs larger than 8 nm. In particular, the binding activities maximized at 4.5 and 5 nm GNPs, dropped to 60% for 3.5 nm, and dropped to 30% for 6 nm GNP.

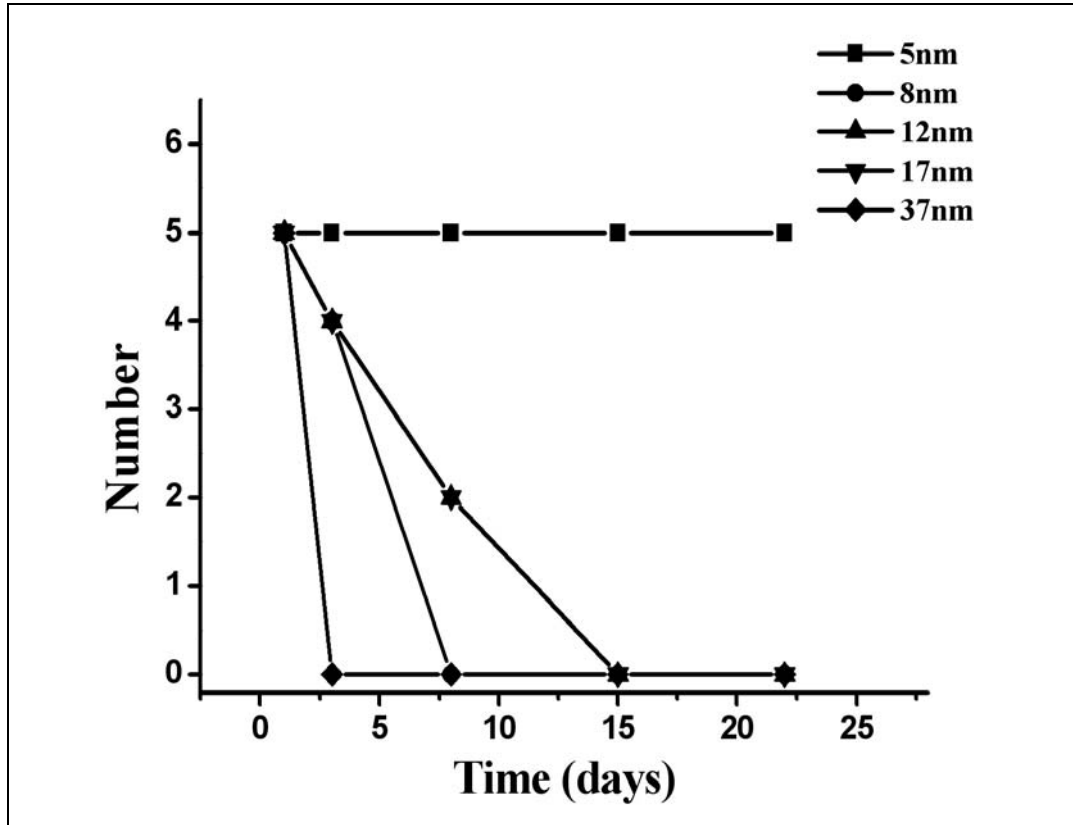


**FIG. 4.1 Survival number for mice immunized with gold nanoparticles**

Gold nanoparticles of 5 nm, 8 nm, 12 nm, 17 nm, and 37 nm at 2.6 mM were mixed with equal volume of adjuvant. One hundred microliters of emulsion were weekly injected into mice. Mice injected with 8 nm (circle), 12 nm (pyramid), 17 nm (triangle), and 37 nm (diamond) GNPs died within 2 weeks. Mice injected with 5 nm (square) GNP survived through the 4-week immunizing procedure.



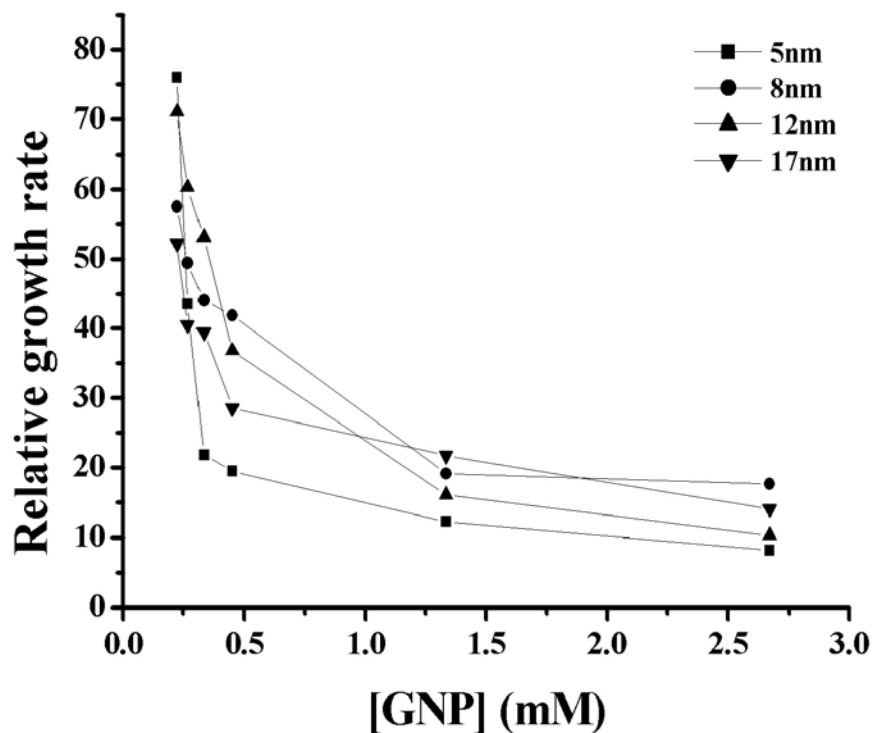


Fig. 4 . 2  $LC_{50}$  measured by MTT assay of NIH-3T3 cell culture

GNPs were added to the growth medium of NIH-3T3 cell culture at indicated concentration and incubated for 12 hours at 37 °C. MTT assay was performed to measure the cell viability.  $LC_{50}$  for GNPs are: 0.15 mM (5 nm GNP, square), 0.17 mM (17 nm GNP, triangle), 0.19 mM (8 nm GNP, circle), and 0.22 mM (12 nm GNP, pyramid).

To examine the specificity of ELISA, competition ELISA was performed using GNPs as competitors in the pre-incubation with antiserum (Figure 3.1). Only 5 nm GNP exhibited competing activity to the antiserum. This binding was unaffected by ZnO nanoparticle (Figure 3.2). Although all GNPs have identical surface for antibody binding, the limited recognition of 4.5 to 5 nm indicated that the flexible range of Fab-Fab angle during antigen recognition was surprisingly restricted.

The lethal effect of GNP injection is intriguing. The uptake of gold nanoparticles by Hela cells maximizes at 50 nm (B. Devika Chithrani, Arezou A. Ghazani, and Warren C. W. Chan Determining the Size and Shape Dependence of Gold Nanoparticle Uptake into Mammalian Cells *Nano Lett.*; 2006; 6(4) pp 662 – 668). However, GNPs exhibited similar cytotoxicity to NIH-3T3 cells in our MTT assay. The injection of GNPs was selectively lethal to mice. Because the survival rate is unrelated to the cytotoxicity of GNPs the lethality of larger GNPs might owe to the inability of mouse immune system to generate antibody that targets and scavenges GNPs from circulation.

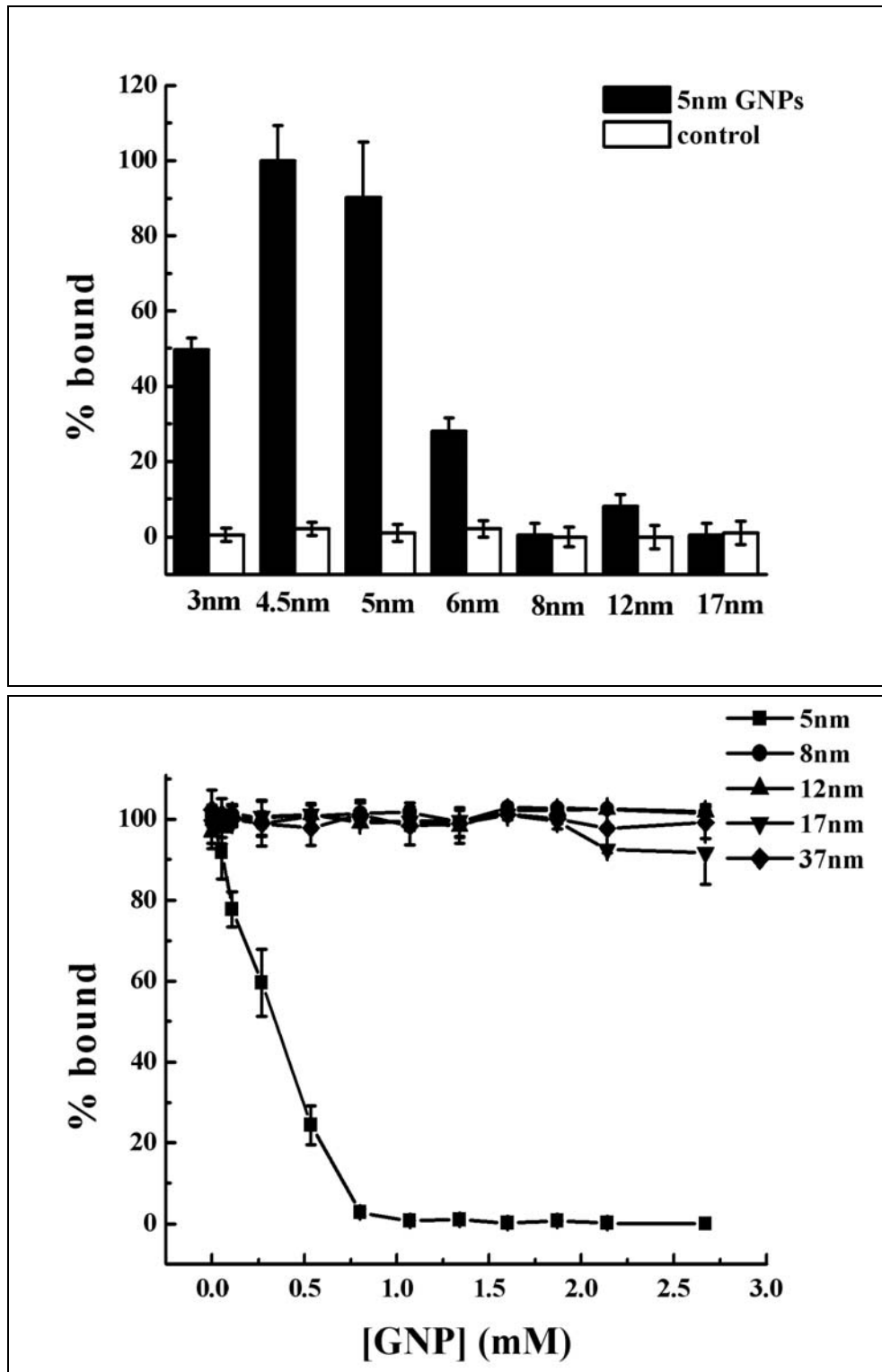


FIG. 4 . 3 Competition ELISA for the binding of anti-5 nm GNP antiserum and 5 GNP

GNPs were applied as competitors. Only 5 nm GNP (square) competed away the binding activity. GNPs of 8 nm (circle), 12 nm (pyramid), and 17 nm (triangle) failed to affect the binding reaction. (B) 20-nm zinc oxide nanoparticle was applied as competitor



## 4. 2 EM imaging of GNP-immunoglobulin-Quantum Dots conjugate

Electron microscopy (EM) imaging might provide structural information of GNP-immunoglobulin complex (GNP-IgG). To assist visualizing GNP-IgG complex we incorporated quantum dots-conjugated goat anti-mouse IgG (QD-IgG) in which quantum dot (QD) has a defined size of 3 nm and could be unambiguously identified under EM. QD-IgG recognizes Fc domain of immunoglobulin. The immuno-precipitation of GNP-IgG and QD-IgG was performed and the precipitate was thoroughly washed, stained with iodine, and examined under EM. The normal serum was co-precipitated with GNP and QD-IgG and served as control.

In the EM images, GNP and QD exhibited solid spheres of 5 nm and 3 nm respectively while protein components showed as blurred mass (Figure 4.1.1). The control experiment exhibited pair-wise particles identified as QD-IgG which might co-precipitated mouse IgG (Figure 4.1.1). Co-precipitation of antiserum, 5 nm GNP, and QD-IgG showed clusters of trio. Each trio was composed of 3 basic components: a grey protein mass of immunoglobulins, a 5 nm GNP and a 3 nm QD (Figure 4.1.2). Higher magnification displayed a GNP-IgGs-QD conformation (Figure 4.1.3).

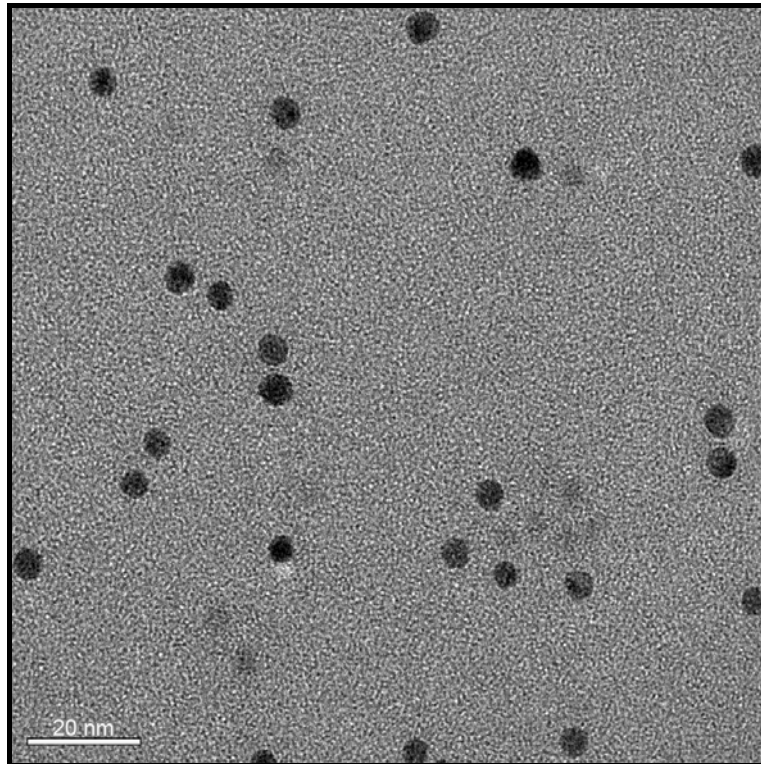


Fig.4.4.1 The control experiment exhibited pair-wise particles identified as QD-IgG which might co-precipitated mouse IgG

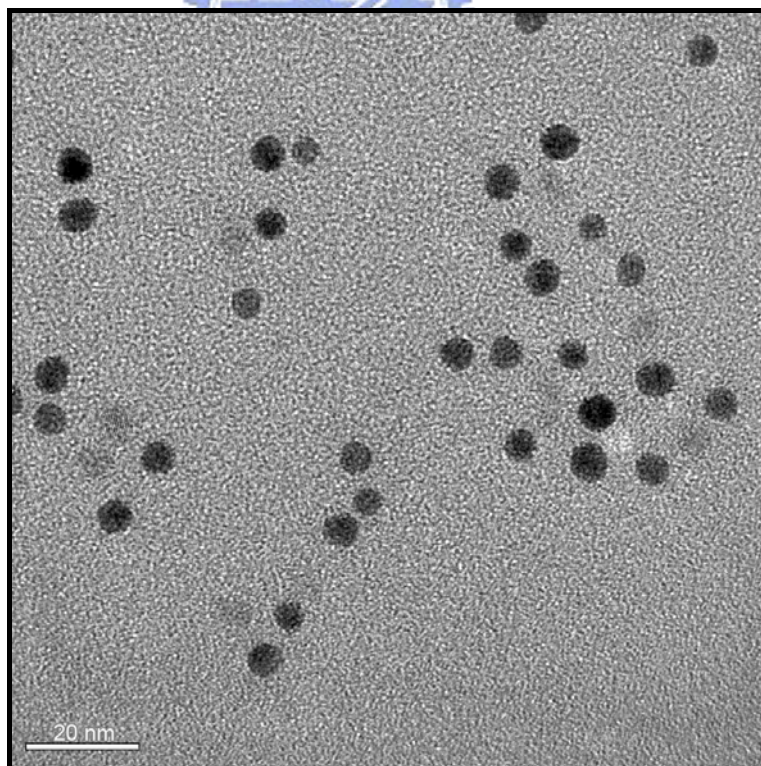


Fig.4.4.2 Each trio was composed of 3 basic components: a grey protein mass of immunoglobulins, a 5 nm GNP and a 3 nm QD.



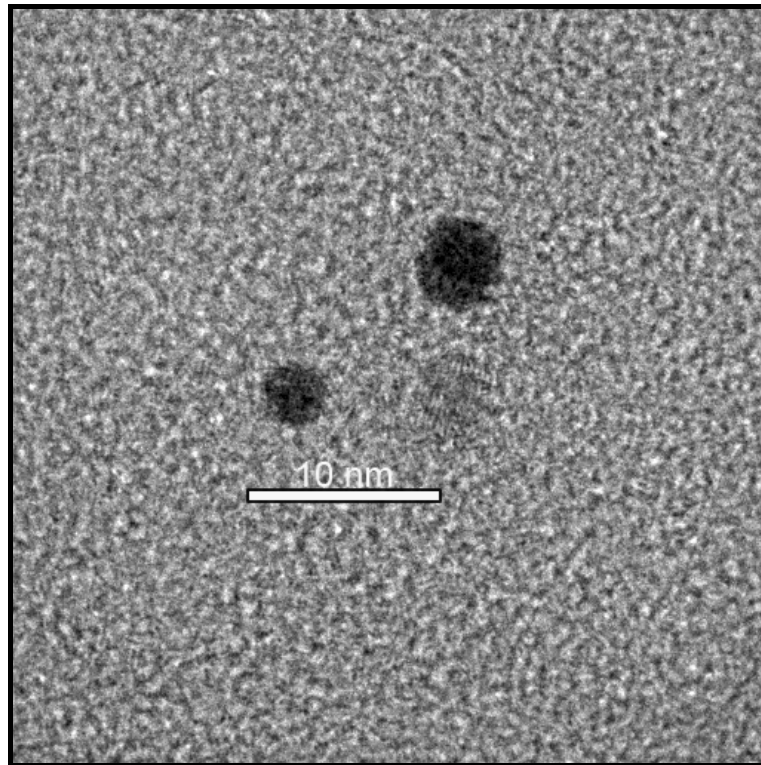


Fig.4.4.3 Higher magnification displayed a GNP-IgGs-QD conformation



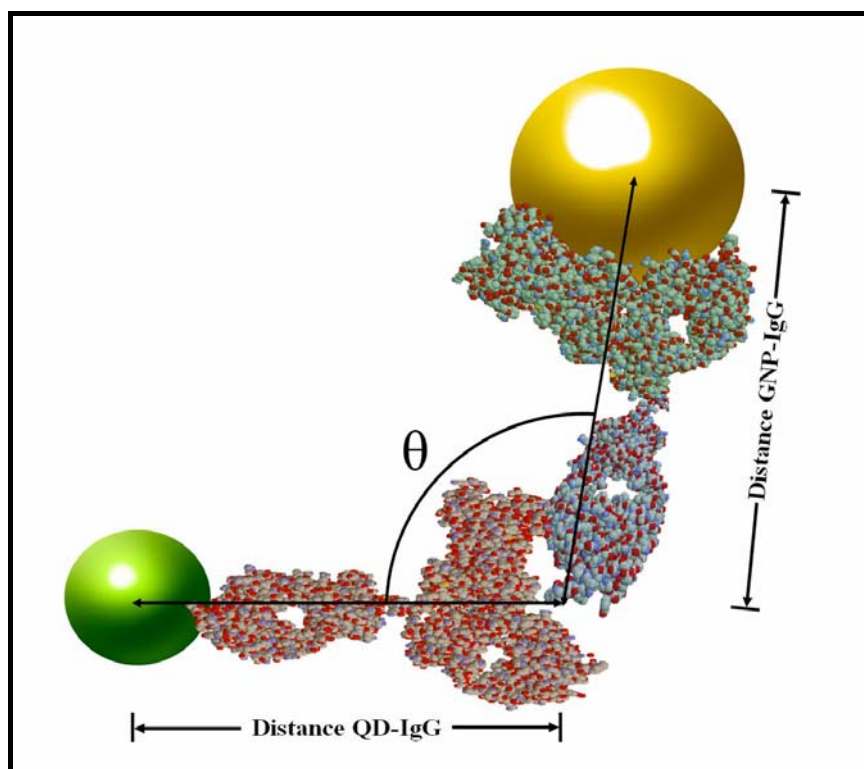


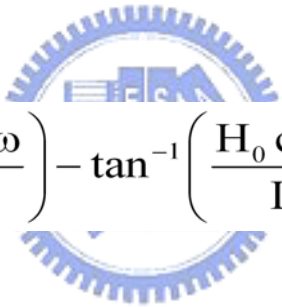
Fig.4.4.4

**FIG. 4. EM image for the co-precipitate of antiserum, 5 nm GNP, and QD-IgG.**

(1) Control serum was precipitated with 5 nm GNP and quantum dots-conjugated antibody. Most clustered spots are composed of two dots separated by approximately 7 nm. The conformation would fit the described QD-IgG. (2) Anti-5 nm GNP antiserum was precipitated with 5 nm GNP and QD-IgG. More complexed pattern was observed. Each cluster can be dissected to three basic components: 5 nm GNP, 3 nm QD, and IgGs. (3) Magnified image from (B) showed a clear GNP-IgGs-QD complex. (4) Molecular model for GNP-IgGs-QD complex.



EM image represented sampling for the conformational space of GNP-(IgGs)-QD complexes. The distances and angles of the triangles were not identical to the distances and angles expected from crystal structure. It is likely that the GNP-IgGs-QD complex may not lie at right angle relative to the incoming electron beam, thus the apparent angles and distances were distorted by tilt angles. To obtain the GNP-(IgGs)-QD angle a ball-and-stick model was proposed (Figure 4.4.4). Assuming that the GNP-(IgGs)-QD triangle with a top angle  $\theta_0$  sitting with a tilt angle  $\omega$  against the horizontal plane (Figure 4.5). The apparent top angle ( $\theta$ ), the apparent distance of GNP-IgG (1), and the apparent distance of QD-IgG (B) can be described as functions of tilt angle ( $\omega$ ):



$$\theta = \pi - \tan^{-1}\left(\frac{H_0 \cos \omega}{L_1}\right) - \tan^{-1}\left(\frac{H_0 \cos \omega}{L_2}\right) \quad (1)$$

$$\theta_0 = \cos^{-1}\left(\frac{H_0}{A_0}\right) + \cos^{-1}\left(\frac{H_0}{B_0}\right) \quad (2)$$

$$A = \sqrt{A_0^2 - H_0^2 (1 - \cos^2 \omega)} \quad (3)$$

$$B = \sqrt{B_0^2 - H_0^2 (1 - \cos^2 \omega)} \quad (4)$$

$$L_1 = \sqrt{A_0^2 - H_0^2} \quad (5)$$

$$L_2 = \sqrt{B_0^2 - H_0^2} \quad (6)$$

Where  $A_0$  is the distance of GNP-IgG (9.0 nm);  $A$  is the apparent distance of GNP-IgG;  $B_0$  is the distance of QD-IgG (7.3 nm);  $B$  is the apparent distance of QD-IgG; and  $H_0$  is the height of the triangle.



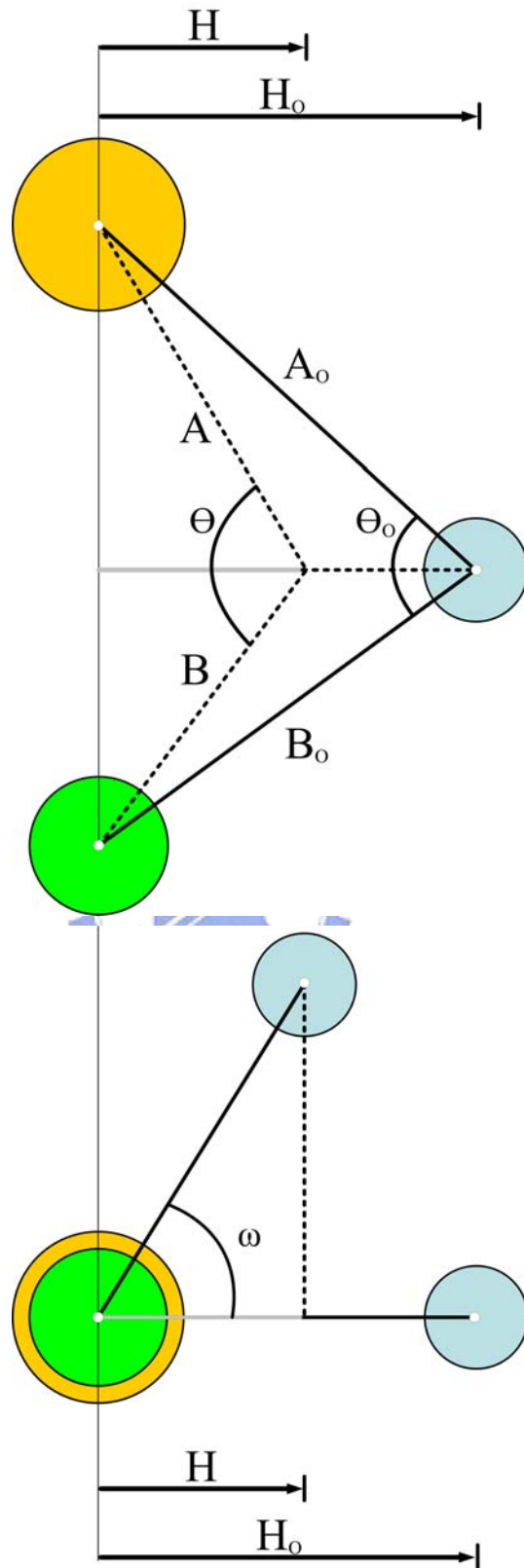


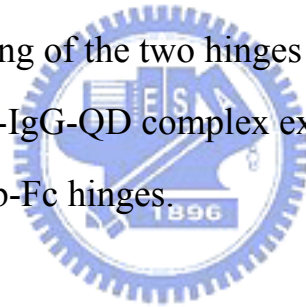
Figure4. 5 Schematic drawing for ball-and-stick model

The drawing shows top view and side view for the GNP-(IgGs)-QD triangle with a top angle  $\theta_0$  sitting at a tilt angle  $\omega$  against the horizontal plane. Yellow circle

represents 5 nm GNP. Green circle represents 3 nm QD. In the drawing  $\theta$  is the apparent top angle;  $A_0$  is the distance of GNP-IgG (9.0 nm);  $A$  is the apparent distance of GNP-IgG;  $B_0$  is the distance of QD-IgG (7.3 nm);  $B$  is the apparent distance of QD-IgG;  $H$  is the apparent height of the triangle; and  $H_0$  is the height of the triangle



Each  $\theta_0$  describes a hyperbolic line in the 3-dimensional space (Figure 4.6) using A, B, and  $\theta$  as axes. These hyperbolic lines of various  $\theta_0$  collectively form a plane. To assign  $\theta_0$  for complexes in the image A, B, and  $\theta$  was measured for each GNP-IgGs-QD complex and plotted in the 3-d space. Deviation of the experimental points away from the plane was observed, probably due to the heterogeneous nature of polyclonal antibodies used in this study, or due to minor denaturation occurred to protein components during the processing of specimen. The theoretical  $\theta_0$  was obtained by projecting each point onto  $\theta_0$  plane (Figure 4.7). The acquired  $\theta_0$  distributed between  $35^\circ$  to  $120^\circ$  and maximized at  $100^\circ$ . It is realized that the flexibility of  $\theta_0$  is shared by two Fab-Fc hinges: anti-GNP IgG and QD-conjugated IgG (Figure 4.8). Furthermore, the observed  $\theta_0$  might not reflect the actual bending of the two hinges due to the blurriness of EM image. Nevertheless, GNP-IgG-QD complex exhibited comparable flexibility as previously reported for Fab-Fc hinges.



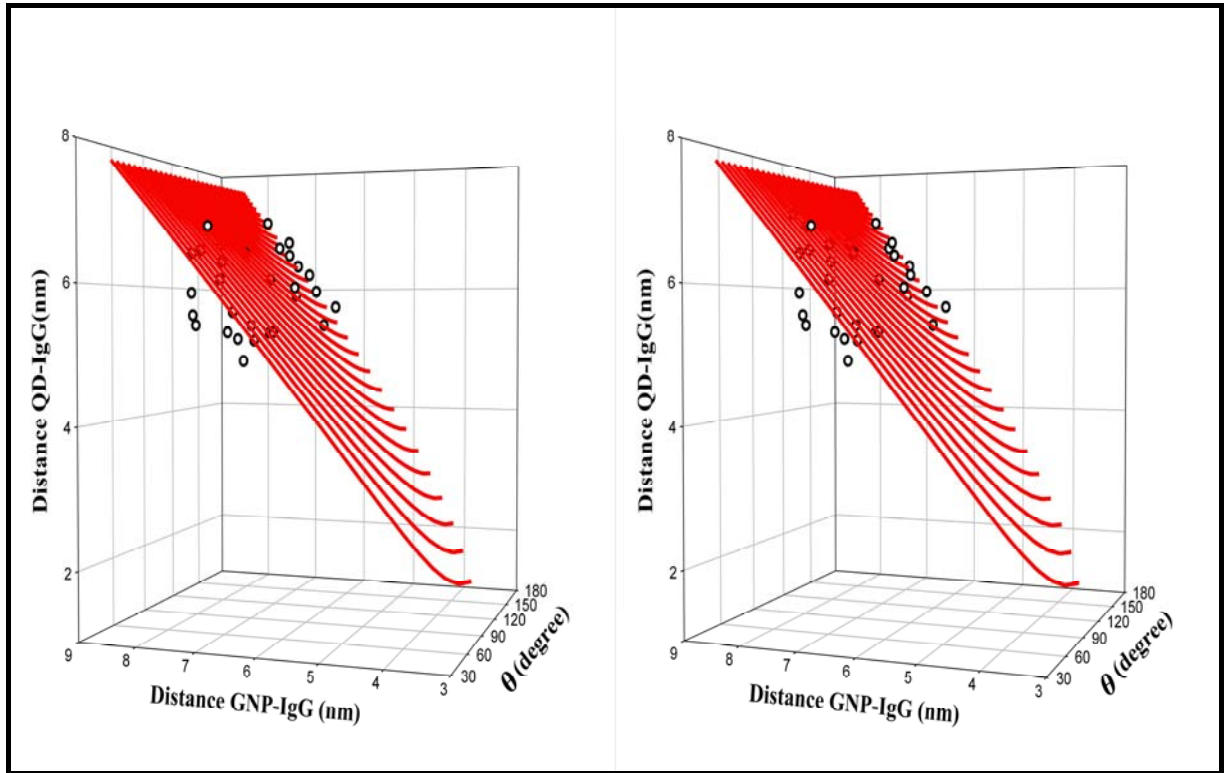


**FIG. 4 .6 Stereo view of 3D plots for the measured angle and distances of GNP-IgGs-QD complexes obtained from cryo-EM Each hyperbolic line represents simulated angle and distances for a specific  $\theta_0$ . Collection of  $\theta_0$  from  $35^\circ$  to  $180^\circ$  forms a plane in the 3D space.**

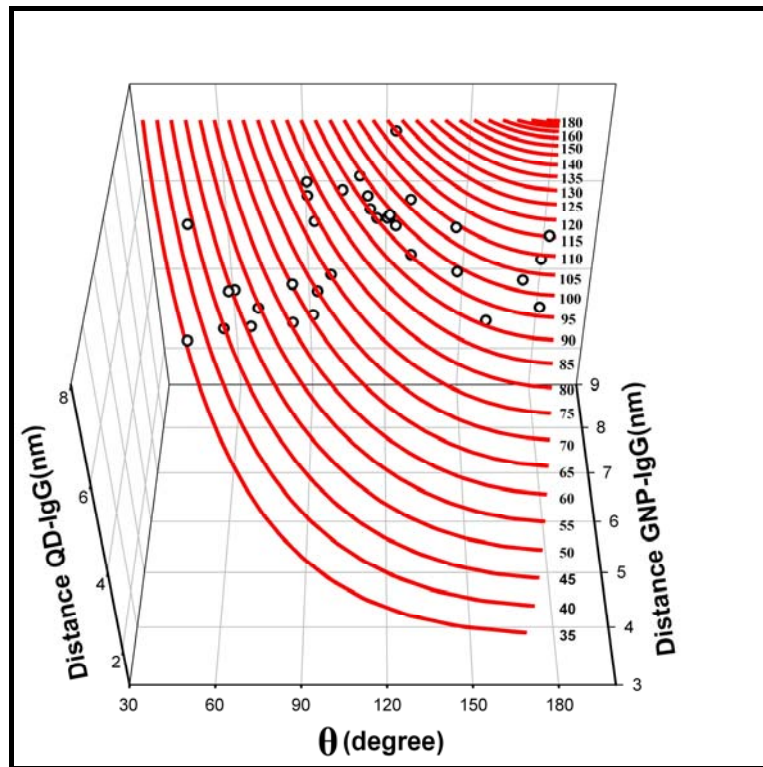


Figure 4.7 Projection of apparent angle and distances of GNP-IgGs-QD complexes on the theoretical  $\theta_0$  plane. Three-dimensional plot is adjusted to a view perpendicular to the theoretical  $\theta_0$  plane. Each point falls on the plane and is assigned to a corresponding  $\theta_0$ .

Because all GNPs have identical surface as epitope for anti-GNP immunoglobulin, the free rotation and movement of Fab arms would allow binding of GNP as large as 17 nm (ref). The inability of antiserum to recognize GNPs larger than 5 nm implied that there is only a limited flexibility for Fab arms for this specific anti-5 nm GNP immunoglobulin. On the other hand, the Fab-Fc hinges were considerably highly flexible that two hinges collectively presented 85 degrees of freedom in the GNP-IgGs-QD complex.

The current study provides a novel platform to measure the functional flexibility of immunoglobulin. The structural information is attained with biochemical and EM images without complicated or tedious procedures. It is foreseeable that such methodology that applied nanoparticles to interfere with biological entities has immense potential to probe the biological world.





# Reference

- [ 1 ] Crystal structure of a neutralizing human IGG against HIV-1: a template for vaccine design. Science. **2001**
- [ 2 ] Cyclophilin a plays distinct roles in human immunodeficiency virus type 1 entry and postentry events, as revealed by spinoculation. J Virol. **2002**
- [ 3 ] Antibiotic therapy for the febrile granulocytopenic cancer patient: combination therapy vs. monotherapy. Rev Infect Dis. **1989**
- [ 4 ] Biochemical features of ceruloplasmin gene mutations linked to aceruloplasminemia. Neuromolecular Med. **2006**
- [ 5 ] Frens, device for quantative measuring of shivering in goats. Lab Anim. **1973**
- [ 6 ] Role of allogeneic bone marrow transplantation for the treatment of myelodysplastic syndromes in childhood. The European Working Group on Childhood Myelodysplastic Syndrome (EWOG-MDS) and the Austria-Germany-Italy (AGI) Bone Marrow Transplantation Registry. Bone Marrow Transplant. **1996**
- [ 7 ] The September 2001 issue of Scientific American discusses exciting developments in the field of nanotechnology and current futuristic applications envisaged for nanomaterials. **2001**
- [ 8 ] Jana, N. R., Gearhart, L. and Murphy, C. J., Chem. Commun., **2001**
- [ 9 ] Chung, S.-W., Markovich, G. and Heath, J. R., J. Phys. Chem., **1998**
- [ 10 ] Esumi, K., Matsuhisa, K. and Torigoe, K., Langmuir, **1995**
- [ 11 ] Broen K. R., Walter, D. G. and Natan, M. J., Chem. Mater., **2000**
- [ 12 ] T. Teranishi, H. Hori and M. Miyake: J. Phys. Chem. B 101 .**1997**
- [ 13 ] Y. Volokitin, J. Sinzig, L. J. de Jong, G. Schmid, M. N. Vargaftik and

- I. I. Moiseev: Nature 384 .1996
- II.
- [ 14 ] A. P. Alivisatos: Science 271 .1996
- [ 15 ] T. Teranishi, I. Kiyokawa and M. Miyake: Adv. Mater. **1998**
- [ 16 ] A. Henglein: J. Phys. Chem. **1993**
- [ 17 ] G. T. Wei, F. K. Liu and C. R. C. Wang: Anal. Chem. 71 **1999**
- [ 18 ] C. A. Mirkin, R. L. Letsinger, R. C. Mucic and J. J. Storhoff: Nature **1999**
- [ 19 ] A. Taleb, C. Petit and M. P. Pileni: Chem. Mater. **1997**
- [ 20 ] S. Peschel and G. Schmid: Angew. Chem. Int. Ed. Eng. **1995**
- [ 21 ] U. Kreibig and M. Vollmer: Optical Properties of Metal Clusters  
Springer-Verlag, Berlin, **1995**
- [ 22 ] Brunger, A. T. (1990). Extension of molecular replacement: a new search strategy based on Patterson correlation Acta Crystallog. sect. A, **1990**
- [ 23 ] Brunger, A. T. 1992. X-PLOR Version 3.1, a System for Crystallography and NMR, Yale University Press, New Haven, CT **1992**
- [ 23 ] Dangl, J. L., Wensel, T. G., Morrison, S. L., Stryer, L., Herzenberg, L. A. & Oi, V. T. (1988). Segmental exhibity and complement of genetically engineered chimeric human, rabbit and mouse antibodies. 1988
- [ 24 ] Deisenhofer, J. 1981. Crystallographic atomic models of a human Fc fragment and its complex with fragment B of protein A from Staphylococcus aureus at 2.9- and 2.8-Å resolution. Biochemistry, **1981**
- [ 25 ] Sarma, R. & Laudin, A. G. (1982). The three-dimensional structure of a human IgG1 immunoglobulin at 4 Å resolution a computer ®t of various structural domains on the electron density map. J. Appl. Crystallog **1982**
- [ 26 ] Satow, Y., Cohen, G. H., Padlan, E. A. & Davies, D. R.(1986).

Phosphocholine binding immunoglobulin Fab McPC603. *J. Mol. Biol.* 190, 593±604. **1986**

- [ 27 ] Sheriff, S., Silvertan, E. W., Padlan, E. A., Cohen, G. H., Smith-Gill, S. J., Finzel, B. C. & Davies, D. R. (1987). Three-dimensional structure of an antibody-antigen complex. *Proc. Natl Acad. Sci. USA*, 84, 8075±8079. **1987**
- [ 28 ] Silvertan, E. W., Navia, M. A. & Davies, D. R. (1977). Three-dimensional structure of an intact human immunoglobulin. *Proc. Natl Acad. Sci. USA*, 74, 5140±5144. **1977**
- [ 29 ] Enzyme-Linked Immunosorbent Assay for Immunoglobulin G and Immunoglobulin A Antibodies to *Shigella flexneri* Antigens INFECTION AND IMMUNITY, May **1979**
- [ 30 ] Ahlstedt, S., J. Holmgren, and L. A. Hanson. 1974. Protective capacity of antibodies against *E. coli* 0 antigen with special reference to the avidity. *Int. Arch. Allergy* 46:470-480. **1974**
- [ 31 ] Avrameas, S. 1969. Coupling of enzymes to proteins with glutaraldehyde. Use of the conjugates for the detection of antibodies. *Immunochemistry* 6:43-52. **1969**
- [ 32 ] Westphal, O., O. Luderitz, and F. Bister. 1952. Über die Extraktion von Bakterien mit Phenol-Wasser. *Z. Naturforsch. Teil B* 7:148-155. **1952**
- [ 33 ] Yardley, J. IL, D. F. Keren, S. R. Hamilton, and G. D. Brown. 1978. Local (immunoglobulin A) immune response by the intestine to cholera toxin and its partial suppression with combined systemic and intra-intestinal immunization. *Infect. Immun.* 19:589-597. **1978**
- [ 34 ] Zollinger, W. D., J. M. Dalrymple, and M. S. Artenstein. 1976. Analysis of parameters affecting the solid phase radioimmunoassay quantitation of antibody to meningococcal antigens. *J. Immunol.* 117:1788-1798. **1976**